PERGAMON

Polyhedron 20 (2001) 3265–3273

POLYHEDRON

www.elsevier.com/locate/poly

Iron(III), cobalt(II,III), copper(II) and zinc(II) complexes of 2-pyridineformamide 3-piperidylthiosemicarbazone

Karen A. Ketcham [a], John K. Swearingen [a], Alfonso Castiñeiras [b], Isabel Garcia [b], Elena Bermejo [b], Douglas X. West [c,*]

[a] *Department of Chemistry, Illinois State University, Normal, IL 61790-4160, USA*
[b] *Departamento de Química Inorgánica, Universidad de Santiago de Compostela, E-15706 Santiago de Compostela, Spain*
[c] *Department of Chemistry, University of Washington, Box 351700, Seattle, WA 98195-1700, USA*

Received 22 March 2001; accepted 21 August 2001

Abstract

Reduction of 2-cyanopyridine by sodium in the presence of 3-piperidylthiosemicarbazide produces 2-pyridineformamide 3-piperidylthiosemicarbazone, HAmpip. Complexes with iron(III), cobalt(II,III) copper(II) and zinc(II) have been prepared and characterized by molar conductivities, magnetic susceptibilities and spectroscopic techniques. In addition, the crystal structures of HAmpip, $[Fe(Ampip)_2]ClO_4$, $[Cu(HAmpip)Cl_2]\cdot CH_3OH$ and $[Zn(HAmpip)Br_2]\cdot C_2H_6SO$ have been determined. Coordination is via the pyridyl nitrogen, imine nitrogen and thiolato or thione sulfur when coordinating as the anionic or neutral ligand, respectively.

Keywords: 2-Pyridineformamide; 3-Piperidylthiosemicarbazone; Iron; Cobalt; Copper; Zinc; Crystal structures

1. Introduction

A new series of N(4)-substituted thiosemicarbazones has been prepared in which the thiosemicarbazone moiety is attached to an amide carbon in an attempt to enhance water solubility. 2-Formyl-, 2-acetyl- and 2-benzoylpyridine N(4)-substituted thiosemicarbazones and many of their metal complexes [1–3] possess substantial in vitro activity against various human tumor lines [4]. However, due to their lack of solubility in aqueous solutions, these thiosemicarbazones and their metal complexes show less promising in vivo activity. Previously, we have reported our studies of metal complexes of 2-pyridineformamide thiosemicarbazone [5–8] and N(4)-methylthiosemicarbazone [9,10]. Some Group 12 metal complexes [11] and nickel(II) complexes [12] of 2-pyridineformamide 3-piperidylthiosemicarbazone have been communicated recently. Here we report the spectral and structural properties of 2-pyridineformamide 3-piperidylthiosemicarbazone, HAmpip, which is depicted in Fig. 1, and a selection of its iron(III), cobalt(II,III) and copper(II) complexes, as well as an additional zinc(II) complex.

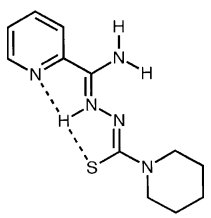

Fig. 1. Drawing of 2-pyridineformamide 3-piperidylthiosemicarbazone, HAmpip.

2. Experimental

2.1. Syntheses and spectral characterization

2-Cyanopyridine was purchased from Aldrich and used as received and 3-piperidylthiosemicarbazide was prepared as described by Scovill [13]. Following the

* Corresponding author. Tel.: +1-206-616-4213; fax: +1-206-685-8665.
E-mail address: westdx@chem.washington.edu (D.X. West).

0277-5387/01/$ - see front matter
PII: S0277-5387(01)00941-X

literature procedure for the reduction of 2-cyanopyridine [14], sodium (0.092 g, 4 mmol) was added to 25 ml of MeOH, which had been dried over $CaSO_4$ (i.e. Drierite), and the solution stirred until complete dissolution occurred. 2-Cyanopyridine (2.6 g, 25 mmol) was then added, and the mixture stirred for 1/2 h followed by addition of 3-piperidylthiosemicarbazide (3.9 g, 25 mmol) in small portions over a period of 1/2 h. On addition of an additional 15 ml of MeOH the mixture was gently refluxed for a minimum of 4 h. Slow evaporation of MeOH produced the yellow HAmpip, IR (KBr, cm^{-1}): 3403, 3218, ν(NH); 1662, δ(NH); 1601, 1582, 1568, ν(CN) + ν(CC); 1006, ν(NN); 861, ν(CS); 607 ρ(py). ^{1}H NMR ($CDCl_3$): N(2)–$\underline{H}$ at $\delta = 13.186$; C–$\underline{H}$ (py) at $\delta = 7.995$, 7.835 and 7.422; N$\underline{H}_2$ at $\delta = 6.4$ ppm; (DMSO): N(2)–$\underline{H}$ at $\delta = 12.69$; C–$\underline{H}$ (py) at $\delta = 8.09$, 7.75 and 7.62; N$\underline{H}_2$ at $\delta = 8.09$ ppm. ^{13}C NMR (DMSO): C(6) at $\delta = 143.67$; C(7) at $\delta = 178.4$ ppm, C(py) at $\delta = 149.63$, 144.25, 138.02, 126.17 and 120.88 ppm; mp, 154–156° C.

The metal complexes were prepared as follows: metal perchlorates, chlorides, acetates or bromides (0.002 mol) in EtOH (30 ml) was mixed with a solution of HAmpip (0.002 or 0.004 mol) in EtOH (30 ml), and the mixture was stirred under reflux for 2 h or longer. The resulting solids were filtered while the solutions were warm, washed with anhydrous ether to apparent dryness and placed on a warm plate at 35 °C until required for characterization. The yields for the various complexes ranged from 57 to 74%. National Chemical Consulting, Inc. of Tenafly, NJ, performed partial elemental analyses and HAmpip and its metal complexes were characterized using techniques and instrumentation reported previously [5–9].

2.2. X-ray data collection, structure solution and refinement

Yellow crystals of HAmpip and brown crystals of $[Fe(Ampip)_2]ClO_4$ were grown from EtOH, brown crystals of $[Cu(HAmpip)Cl_2]\cdot MeOH$ from 1:1 (v/v) mixture of MeOH and MeCN and yellow crystals of $[Zn(HAmpip)Br_2]\cdot DMSO$ from DMSO. The crystals were mounted on glass fibers and used for data collection. Data for $[Fe(Ampip)_2]ClO_4$ and $[Cu(HAmpip)Cl_2]\cdot MeOH$ were obtained with an Enraf–Nonius MACH3 diffractometer, data for HAmpip were obtained with an Enraf–Nonius CAD4 diffractometer radiation and data for $[Zn(HAmpip)Br_2]\cdot DMSO$ were obtained with a Bruker SMART CCD 1000 diffractometer. Data for $[Zn(HAmpip)Br_2]\cdot DMSO$ were processed with SAINT [15] and corrected for absorption using SADABS [16]. The four structures were solved by direct methods [17], which revealed the position of all non-hydrogen atoms, and refined by a full-matrix least-squares procedure on F (i.e. $[Cu(HAmpip)Cl_2]\cdot MeOH$) or F^2 (i.e. HAmpip, $[Fe(Ampip)_2]ClO_4$ and $[Zn(HAmpip)Br_2]\cdot DMSO$) using anisotropic displacement parameters [18]. The hydrogens attached to nitrogens in the four structures were located from difference Fourier maps and refined isotropically. The remaining hydrogens were located in their calculated positions (C–H 0.93–0.97 Å) and refined using a riding model. Atomic scattering factors are from 'International Tables for X-ray Crystallography' [19] and molecular graphics are from PLATON99 [20]. Summaries of crystal and intensity collection data for the four compounds are given in Table 1.

3. Results and discussion

The bond distances for HAmpip and its complexes are given in Table 2 and their bond angles in Table 3. Table 4 lists the hydrogen bonding interactions and Table 5 the mean plane data and angles between planes. Figs. 2–5 show the ORTEP diagrams of HAmpip, $[Fe(Ampip)_2]ClO_4$, $[Cu(HAmpip)Cl_2]\cdot MeOH$ and $[Zn(HAmpip)Br_2]\cdot DMSO$, respectively.

3.1. HAmpip, structural characterization

In contrast to 2-pyridineformamide thiosemicarbazone, HAm4DH [5], which possesses two crystallographically independent molecules and 2-pyridineformamide N(4)-methylthiosemicarbazone, HAm4M [10], with four crystallographically independent molecules, HAmpip has a single unique molecule, Fig. 2. While HAm4DH and HAm4M have an E conformation with respect to the imine carbon–nitrogen bond, C16–N12, and the thiosemicarbazone moiety directed away from the pyridine ring, HAmpip is in the bifurcated E′ conformation like 2-acetylpyridine 3-hexamethyleneiminylthiosemicarbazone, HAchexim [21]. Although the non-bonding distance between N2 and S1 is somewhat longer than N2···N1, the H···N1 and H···S1 distances are nearly the same. As expected, because of the different structural forms, the greatest differences in the bond distances between HAmpip and HAm4M are in the thioamide part of the thiosemicarbazone moiety. For example, C17–S1, which is formally a single bond in HAmpip, has a bond distance of 1.730(2) Å, but in HAm4M [10] it averages 1.699(5) Å and is formally a double bond. The bond distances and angles of HAmpip are similar to those reported for the bifurcated HAchexim [21] with the following differences: C17–S1, 1.730(2) Å compared to 1.70(1) Å for HAchexim and C16–N12–N13, 121.3(2)° compared to 125(1)° for HAchexim. Also, in bifurcated HAchexim the H2···S1 non-bonding distance is actually less than the H2···N1 distance [21].

Table 1
Crystal data and structure refinement parameters for HAmpip, $[Fe(Ampip)_2]ClO_4$, $[Cu(HAmpip)Cl_2]\cdot CH_3OH$ and $[Zn(HAmpip)Br_2]\cdot C_2H_6SO$

Empirical formula	$C_{12}H_{17}N_5S$	$C_{24}H_{32}N_{10}O_4S_2ClFe$	$C_{13}H_{21}Cl_2CuN_5OS$	$C_{14}H_{23}Br_2N_5OS_2Zn$
Formula weight	263.37	680.0	429.85	566.68
Color; habit	yellow; plate	dark brown; prism	blue; prism	yellow; prism
Crystal size (mm)	$0.35\times0.20\times0.05$	$0.20\times0.20\times0.20$	$0.20\times0.12\times0.12$	$0.22\times0.09\times0.05$
Radiation, λ (Å)	Cu Kα, 1.54184	Mo Kα, 0.71073	Mo Kα, 0.71073	Mo Kα, 0.71073
Temperature (K)	293(2)	293(2)	293(2)	293(2)
Crystal system	monoclinic	monoclinic	triclinic	triclinic
Space group	$P2_1/n$ (#14)	$P2_1/a$ (#14)	$P\bar{1}$ (#2)	$P\bar{1}$ (#2)
Unit cell dimensions				
a (Å)	11.1573(2)	15.534(9)	7.554(8)	9.2126(11)
b (Å)	8.6844(3)	12.640(2)	10.056(9)	9.5176(12)
c (Å)	14.5955(2)	17.072(7)	12.248(7)	12.5062(15)
α (°)	90	90	81.59(5)	102.756(3)
β (°)	109.543(2)	115.95(4)	79.66(8)	93.101(3)
γ (°)	90	90	90.55(13)	94.958(3)
V (Å^3)	1332.75(6)	3014.08(4)	905.5(13)	1062.5(2)
Z	4	4	2	2
D_{calc} (Mg m^{-3})	1.313	1.499	1.577	1.771
Absorption coefficient (mm^{-1})	2.078	0.777	1.626	5.126
$F(000)$	560	1412	442	564
θ range (°)	4.36–76.06	1.33–24.65	1.71–27.47	1.67–28.07
Index ranges	$-13\le h\le14$, $0\le k\le10$, $-18\le l\le0$	$0\le h\le20$, $0\le k\le16$, $-22\le l\le$	$-9\le h\le9$, $-13\le k\le13$, $-15\le l\le15$	$-12\le h\le12$, $-12\le k\le7$, $-15\le l\le16$
Absorption correction	Ψ-scan	Ψ-scan	Ψ-scan	SADABS
Max/min transmission	0.974/0.768	1.000/0.984	0.7925/0.6412	1.000/0.824
Reflections collected	2878	7202	4455	5759
Independent reflections R_{int}	2769, 0.0274	4905, 0.0173	4138, 0.0287	4044, 0.0565
Final R indices [$I>2\sigma I$)]	$R_1=0.0410$	$R=0.0475$	$R=0.0787$	$R=0.0543$
	$wR_2=0.0995$	$wR=0.1184$	$wR=0.0882$	$wR=0.0957$
R indices (all data)	$R_1=0.0833$	$R=0.0704$	$R=0.1277$	$R=0.1802$
	$wR_2=0.1173$	$wR=0.1441$	$wR=0.1189$	$wR=0.1183$
Goodness-of-fit	1.010	1.110	1.014	0.746
Largest difference peak/hole (e Å^{-3})	0.256/−0.229	0.765/−0.884	1.134/−1.300	0.535/−0.538

Table 2
Bond lengths (Å) for HAmpip, $[Fe(Ampip)_2]ClO_4$, $[Cu(HAmpip)Cl_2]\cdot CH_3OH$ and $[Zn(HAmpip)Br_2]\cdot C_2H_6SO$

Bond	HAmpip	$[Fe(Ampip)_2]ClO_4$	$[Cu(HAmpip)Cl_2]$	$[Zn(HAmpip)Br_2]$
M–S1		2.2299(18), 2.2211(14)	2.262(2)	2.416(3)
M–N11		1.998(3), 2.008(3)	2.019(5)	2.157(7)
M–N12		1.911(3), 1.913(3)	1.965(5)	2.128(7)
M–C11(Br1)			2.226(3)	2.4246(14)
M–C12(Br2)			2.691(3)	2.4501(14)
S1–C17	1.730(2)	1.763(4), 1.764(4)	1.711(6)	1.695(10)
C16–N12	1.300(3)	1.305(5), 1.307(5)	1.300(7)	1.283(10)
N12–N13	1.375(2)	1.384(4), 1.379(4)	1.401(6)	1.379(8)
N13–C17	1.340(3)	1.320(5), 1.317(5)	1.357(7)	1.338(10)
C17–N14	1.358(3)	1.349(5), 1.347(5)	1.331(8)	1.331(11)
C16–N15	1.329(3)	1.355(5), 1.355(6)	1.318(7)	1.321(12)

One of the NH_2 hydrogens (i.e. H15B) forms an intermolecular hydrogen bond with the sulfur of a neighboring molecule. The distance and angle of this interaction for HAmpip, 3.343(2) Å and 165°, are similar to 3.357(5) Å and 171(5)° reported earlier for HAm4M [10], as well as numerous heterocyclic thioureas [22]. C16–N12–N13–C17–S1–N14 has a mean plane deviation of 0.0500 Å compared to averages of 0.0373 and 0.0417 Å for HAm4M and HAm4DH and forms an angle of 11.95(13)° with the pyridine ring mean plane compared to averages of 14.1(4) and 6.76(13)° for HAm4M [10] and HAm4DH [5].

3.2. $[Fe(Ampip)_2]ClO_4$, structural and spectral characterization

Each Ampip anion is coordinated as a NNS tridentate ligand, and the complex has a meridional arrangement as shown in Fig. 3, which is favored because of the planarity of the conjugated ligand system. The two Ampip ligands have essentially equivalent Fe–S bond distances and the Fe–N (imine) bonds are shorter than Fe–N (pyridine) bonds. Coordination lengthens the thiosemicarbazone moiety's C17–S1 bond from 1.730(2) Å in HAmpip to an average of 1.763(4) Å, and shortens the N3–C8 bond from 1.340(3) Å to an average of 1.319(5) Å in $[Fe(Ampip)_2]ClO_4$. This increase in the former and decrease in the latter is not as large as when the uncomplexed thiosemicarbazone is in a conformation other than the bifurcated E′ (i.e. E or Z with respect to the imine bond). None of the other thiosem-

Table 3
Bond angles (°) for HAmpip, $[Fe(Ampip)_2]ClO_4$, $[Cu(HAmpip)Cl_2]\cdot CH_3OH$ and $[Zn(HAmpip)Br_2]\cdot C_2H_6SO$

Bond	HAmpip	$[Fe(Ampip)_2]ClO_4$	$[Cu(HAmpip)Cl_2]$	$[Zn(HAmpip)Br_2]$
S1–M–S11		96.60(6)		
S1–M–N11		162.71(10), 163.32(10)	163.63(15)	150.4(2)
S1–M–N12		83.90(11), 84.17(10)	84.24(16)	79.1(2)
S1–M–N31		91.04(10), 92.23(10)		
S1–M–N32		94.89(11), 94.77(10)		
N11–M–N12		80.56(14), 80.42(13)	77.8(1)	73.2(3)
N11–M–N31		84.49(13)		
N11–M–N32		100.80(14), 100.78(13)		
N12–M–N32		178.30(13)		
S1–M–Cl1(Br1)			95.14(10)	103.91(8)
N11–M–Cl1(Br1)			97.77(16)	95.61(19)
N12–M–Cl1(Br1)			160.66(17)	110.99(19)
S1–M–Cl2(Br2)			100.83(9)	97.40(8)
N11–M–Cl2(Br2)			86.39(16)	95.2(2)
N12–M–Cl2(Br2)			97.39(18)	135.69(19)
C11(Br1)–M–Cl2(Br2)			101.69(11)	112.70(5)
M–S1–C17		96.32(15), 96.27(14)	98.8(1)	99.7(4)
M–N12–C16		118.3(3), 118.5(3)	118.4(4)	120.0(7)
M–N12–N13		125.1(2), 125.0(2)	120.5(3)	119.4(6)
N15–C16–N12	120.0(2)	123.6(4), 122.3(4)	126.4(5)	126.9(10)
C15–C16–N12	117.3(2)	113.8(3), 113.6(3)	113.1(5)	114.3(9)
C16–N12–N13	121.3(2)	116.5(3), 116.2(3)	120.7(4)	119.6(8)
N12–N13–C17	111.61(19)	111.5(3), 111.6(3)	116.3(4)	119.8(8)
N13–C17–N14	115.2(2)	118.6(4), 118.8(4)	118.4(5)	119.6(9)
N13–C17–S1	123.87(16)	122.3(3), 122.5(3)	120.0(4)	120.7(8)
N14–C17–S1	120.98(17)	119.1(3), 118.6(3)	121.5(4)	119.6(8)

Table 4
Hydrogen bonding interactions (Å, °) for HAmpip, $[Fe(Ampip)_2]ClO_4$, $[Cu(HAmpip)Cl_2]\cdot CH_3OH$ and $[Zn(HAmpip)Br_2]\cdot C_2H_6SO$

Compound	D–H···A	*d*(D–H)	*d*(H···A)	*d*(D···A)	∠(DHA)
Hampip[a]	N15–H15B···S1 # 1	0.86(3)	2.50(3)	3.343(2)	165(3)
	N12–H12···S1	0.90(3)	2.30(3)	2.816(2)	116(2)
	N12–H12···N11	0.903)	2.27(3)	2.632(3)	103(2)
$[Fe(Ampip)_2]ClO_4$[b]	N15–H15A···O3 # 1	0.77(5)	2.33(6)	3.013(7)	148(5)
	N15–H15A···O4 # 1	0.77(5)	2.86(5)	3.305(12)	120(5)
	N15–H25B···O4 # 2	0.84(6)	2.62(6)	3.215(13)	129(5)
	N35–H35B···O2 # 3	0.68(6)	2.47(6)	3.015(8)	138(6)
$[Cu(HAmpip)Cl_2]$[c]	N13–H13···Cl2 # 1	0.86	2.46	3.290(6)	161.3
	N15–H15A···Cl2 # 1	0.86	2.33	3.156(6)	160.3
	N15–H15B···Cl2 # 2	0.86	2.43	3.249(6)	158.9
$[Zn(HAmpip)Br_2]$[d]	N13–H13···O1	0.86	2.13	2.976(10)	166.3
	N15–H15A···O1	0.75(9)	2.02(10)	2.747(11)	165(12)
	N15–H15A···S22	0.75(9)	2.98(10)	3.624(12)	146(11)
	N15–N15B···Br2 # 1	0.87(9)	2.91(9)	3.588(9)	136(8)

Symmetry transformations used to generate equivalent atoms: (a) # 1: $-x, +1/2, y+1/2, -z+1/2$. # 1: $x, y+1, z$; # 2: $-x+2, -y, -z+1$; # 3: $x-1/2, -y-1/2, z$. (b) 1: $-x, -y+2, -z+2$; # 2: $x-1, y, z$. (c) # 1: $-x+2, -y+2, -z+1$.

Table 5
Root mean squared planes for HAmpip, $[Fe(Ampip)_2]ClO_4$, $[Cu(HAmpip)Cl_2]\cdot CH_3OH$ and $[Zn(HAmpip)Br_2]\cdot C_2H_6SO$

Compound	Plane	Rms dev.	Largest dev.	Angle with previous plane
Hampip	C16–N12–N13–C17–N14–S1	0.0500	N12, 0.0941(18)	
	N11–C11–C12–C13–C14–C15	0.0073	C12, 0.0091(26)	11.95(13)
$[Fe(Ampip)_2]ClO_4$	S1–N11–N12–N32	0.0769	N12, 0.0879(15)	
	C16–N12–N13–C17–N14–S1	0.0270	N12, 0.0461(26)	7.30(8)
	N11–C11–C12–C13–C14–C15	0.0053	C11 0.0086(29)	6.47(12)
	N31–C31–C32–C33–C34–C35	0.0039	C31, 0.0064(26)	80.29(14)
	C36–N32–N33–C37–N34–S2	0.0152	N33, 0.0238(31)	3.57(21)
	S2–N31–N32–N12	0.0668	N32, 0.0763(16)	4.91(16)
$[Cu(HAmpip)Cl_2]$	C11–S1–N12–N11–Cu1	0.1345	Cu1, 0.1992(17)	
	C16–N12–N13–C17–S1–N14	0.0378	N12, 0.0685(43)	9.61(20)
	N11–C11–C12–C13–C14–C15	0.0059	C12, 0.0098(52)	3.29(31)
$[Zn(HAmpip)Br_2]$	Br2–S1–N12–N11	0.2211	N12, 0.2779(35)	
	C16–N12–N13–C17–N14–S1	0.0211	N13, 0.0294(64)	18.59(30)
	N11–C11–C12–C13–C14–C15	0.0054	C12, 0.0087(69)	2.64(48)

icarbazone bonds change significantly on coordination, but the amide C16–N15 bond changes from 1.329(3) Å in HAmpip to an average of 1.355(6) Å for the two ligands in $[Fe(Ampip)_2]ClO_4$. Hydrogen bonding between the NH_2 hydrogens and oxygens of the disordered perchlorate anion, Table 4, causes considerable distortion; the shortest Cl–O bond is 1.281(6) Å and the longest 1.431(10) Å. The thiosemicarbazone ligands hydrogen bond differently with the S1 ligand having a greater number of interactions.

The smallest *cis* bond angles about the iron center occur for donor atoms in the same ligand {e.g. N11–Fe–N12, 80.56(14) and N12–Fe–S1, 83.90(11)°}. The *trans* angle involving the two imine nitrogens, N12–Fe–N32, is 178.30(13)° and is marginally closer to 180° than found for $[Fe(Am4M)_2]ClO_4$, 177.6(3)° [10]. The planes N11–N12–S1–N32 and N31–N32–S2–N12, have mean plane deviations of 0.0769 and 0.0668 Å, respectively, and for each plane the imine nitrogens, N12 and N32, deviate from the plane to the greatest extent; the pyridine nitrogens are most out of the plane for $[Fe(Am4M)_2]ClO_4$ [10]. The Fe(III) is 0.576(15) and 0.451(15) Å from the two coordination planes. The angle between thiosemicarbazone moieties is 86.56(4.77)° further indicating that the deviation from a regular octahedron is small except for the bite angle requirements of the tridentate ligands.

The dark brown $[Fe(Ampip)_2]ClO_4$ is low spin, Table 6, in agreement with previously studied iron(III) complexes with two heterocyclic thiosemicarbazone ligands [10,23], and has a molar conductivity in DMF (1×10^{-3} M) of 68.5 $ohm^{-1}\,cm^2\,mol^{-1}$ indicating a 1:1 electrolyte [24]. Loss of hydrogen from the thiosemicarbazone moiety and coordination in $[Fe(Ampip)_2]ClO_4$ results in ν(CN) decreasing 27 cm^{-1}, ν(CS) decreasing 99 cm^{-1} and ρ(py) increasing 30 cm^{-1}, consistent with the mode of coordination shown in the crystal structure determination. The assignments of $\nu(FeN) = 455$ cm^{-1} and $\nu(FeS) = 354$ cm^{-1} are consistent with previously studied bis(heterocyclic thiosemicarbazone)iron(III) complexes [10,23].

The rhombic distortion in the ESR spectrum is common for low spin bis(heterocyclic thiosemicarbazone)iron(III) complexes [10,23], as well as iron(III)

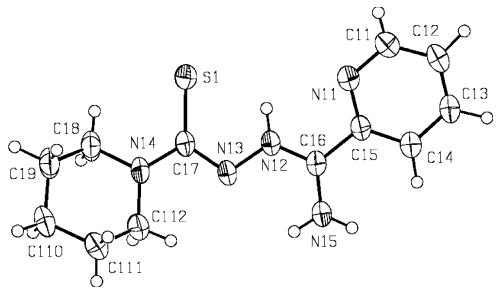

Fig. 2. ORTEP diagram of HAmpip at 50% probability showing numbering system.

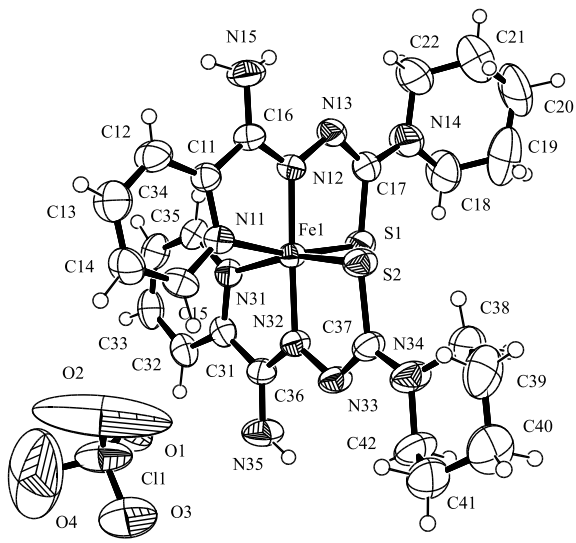

Fig. 3. ORTEP diagram of $[Fe(Ampip)_2]ClO_4$ at 50% probability.

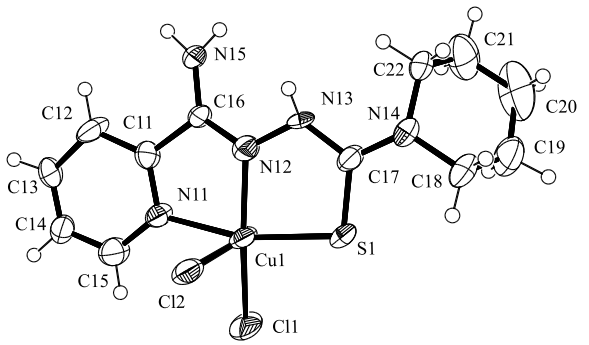

Fig. 4. ORTEP diagram of $[Cu(HAmpip)Cl_2]$ at 50% probability.

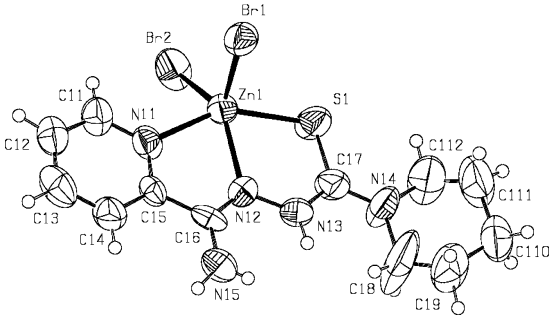

Fig. 5. ORTEP diagram of $[Zn(HAmpip)Br_2]$ at 50% probability.

Table 6
Colors, partial elemental analyses, magnetic susceptibilities, and molar conductivities of the metal ion complexes of 2-pyridineformamide 3-piperidylthiosemicarbazone

Compound	Color	Found (Calc. %)		μ [a]
		C	H	
Hampip [b]	bright yellow	54.2(54.7)	5.9(6.5)	
$[Fe(Ampip)_2]ClO_4$ [c]	dark brown	39.9(40.3)	4.2(5.1)	1.5
$[Co(Ampip)_2]ClO_4$	red brown	41.7(42.2)	4.7(4.7)	0
[Co(Ampip)Cl]	dark brown	39.7(40.4)	4.3(4.5)	2.7
[Cu(Ampip)OAc]	green	43.5(43.7)	4.7(5.0)	2.0
[Cu(Ampip)Cl] [d]	dull brown	39.9(39.9)	4.3(4.5)	1.8
$[Zn(HAmpip)Br_2]$ [e]	yellow	29.12(29.50)	5.6(3.5)	

[a] B.M.
[b] %N = 26.8(26.6).
[c] %N = 18.7(19.6).
[d] %N = 19.1(19.4).
[e] %N = 14.1(14.3), S = 6.4(6.6)

complexes with sp^2 nitrogen donor atoms; this behavior has been reported for Schiff base, as well as porphyry iron(III) complexes [25]. The three g-values in the room temperature rhombic spectrum of $[Fe(Ampip)_2]ClO_4$ powder, 1.992, 2.127 and 2.198 compared to 2.000, 2.136 and 2.206 for $[Fe(Am4M)_2]ClO_4$ [10], is consistent with more covalent bonding in the present complex. The relatively small deviation of the anisotropic g-values from 2.0 suggest the electronic configuration of the ground state is $(d_{xz})^2(d_{yz})^2(d_{xy})^1$ [1,26] (Table 7).

3.3. $[Co(Ampip)_2]ClO_4$ and [Co(Ampip)Cl], spectral characterization

Oxidation to cobalt(III) occurs during preparation of complexes of heterocyclic thiosemicarbazones using cobalt(II) salts with weakly coordinating anions [27,28]. The mechanism of this oxidation has not been proposed, but it is known that preparations with the analogous semicarbazones do not produce cobalt(III) salts [23a]. Thus, $[Co(Ampip)_2]ClO_4$ is diamagnetic, a 1:1 electrolyte [24] and has infrared bands similar to those of $[Fe(Ampip)_2]ClO_4$. The solid state electronic spectrum has absorption bands consistent with approximately octahedral cobalt(III), and we suggest the following assignments: $^1A_{1g} \rightarrow {}^1T_{1g}$, 21 900 cm^{-1}; $^1A_{1g} \rightarrow {}^1T_{2g}$, 25 920 cm^{-1}; $^1A_{1g} \rightarrow {}^3T_{1g}$, 6860 cm^{-1} and $^1A_{1g} \rightarrow {}^3T_{2g}$, 15 960 cm^{-1}. Assignment of the two higher energy bands is complicated by overlap with the more intense intraligand and charge transfer bands (Table 8). However, these assigned energies allow calculation of $Dq = 2320$ cm^{-1}, $B = 694$ cm^{-1}, $\beta = 0.63$ and $C = 4860$ cm^{-1}, which indicate that Ampip provides more covalent bonding and a stronger ligand field than Am4M in $[Co(Am4M)_2]ClO_4$, $Dq = 2{,}220$ cm^{-1}, $B = 820$ cm^{-1}, $\beta = 0.75$ and $C = 4{,}450$ cm^{-1} [10]. Also the ligand field is larger and the covalency greater than found for $[Co(Acpip)_2]ClO_4$, where Acpip is the anion of 2-acetylpyridine 3-piperidylthiosemicarbazone [29].

The complex prepared with 2-pyridineformamide N(4)-methylthiosemicarbazone, $[Co(HAm4M)Cl_2]$, is five-coordinate with the neutral ligand occupying three sites [10], but as is often the case [2,3,21,29,30], N(4)-dialkyl- and 3-azacyclothiosemicarbazones lose the thiosemicarbazone hydrogen to coordinate as anions. Interestingly, a number of years ago the yellow–green complex isolated from a preparation with cobalt(II) chloride and 2-acetylpyridine 3-piperidylthiosemicarbazone was found to have cobalt(III) cations and tetrachlorocobaltate(II) anions, $[Co(Acpip)_2]_2[CoCl_4]$ [29]. However, the dark brown [Co(Ampip)Cl] is four-coordinate and unlikely to approach tetrahedral symmetry because of the necessary planarity of Ampip. In agreement, the magnetic susceptibility, 2.7 B.M., suggests considerable distortion toward a planar arrangement. Unfortunately, we and others have failed to produce suitable crystals to determine the structure of cobalt(II) thiosemicarbazone complexes with this stoichiometry.

3.4. $[Cu(HAmpip)Cl_2]$, structural and spectral characterization

The neutral HAmpip ligand is coordinated via its pyridine nitrogen, imine nitrogen and thione sulfur atoms, which along with Cl1 make up a basal plane, and Cl2 occupies the apical position of an approximately square pyramidal structure, Fig. 4. The geomet-

Table 7
ESR spectral parameters of the solid copper(II) and iron(III) complexes of 2-pyridineformamide 3-piperidylthiosemicarbazone

Compound	Temperature	g_1	g_2	g_3	g_{av}
$[Fe(Ampip)_2]ClO_4$	RT	2.198	2.127	1.992	2.106
	77 K	2.201	2.138	2.000	2.113
[Cu(Ampip)OAc]	RT	2.188	2.059	2.034	2.093
	77 K	2.199	2.065	2.034	2.099
[Cu(Ampip)Cl]	RT	2.136	2.069	2.042	2.082
	77 K	2.136	2.069	2.041	2.082
$[Cu(HAmpip)Cl_2]$	RT	2.158	2.046	2.036	2.080
	77 K	2.159	2.046	2.035	2.080

rical parameter τ, i.e. $\tau = (\beta - \alpha)/60$ [31], where α and β are the N11–Cu–S1 and Cl1–Cu–N2 bond angles, respectively, has a value of 0.05. Therefore, the distortion from square pyramid stereochemistry is small and is comparable to the values of 0.09 and 0.05 found for five-coordinate complexes prepared with 2-formylpyridine N(4)-cyclohexyl- and 2-formylpyridine 3-(4-methylpiperazine)thiosemicarbazone, $[Cu(HFo4CHex)Cl_2]$ and $[Cu(HFoppz4M)Cl_2]$, respectively; the latter is the first heterocyclic thiosemicarbazone with a coordinated thiol function [32]. For $[Cu(HBz4P)Cl_2]$, where HBz4P is 2-benzoylpyridine N(4)-propylthiosemicarbazone [3], the Cl1–Cu–N12 is larger, 165.0(1)° than N11–Cu–S1, 160.7(1)° and calculation of τ on interchanging the assignments gives $\tau = 0.07$ in good agreement with the above complexes. In $[Cu(HAmpip)Cl_2]$ the apical Cl_2 is further from the copper center than Cl1 by 0.47 Å, which is within the 0.38–0.51 Å range found the previously studied five-coordinate copper(II) complexes [3,32]. Cl2 makes angles of approximately 100° with the larger planar donor atoms (i.e. S, Cl1), a lesser angle with N12 {i.e. 97.39(18)° for $[Cu(HAmpip)Cl_2]$, compared to 94.1(1) and 93.57(11)° for $[Cu(HBz4P)Cl_2]$ [3] and $[Cu(HFo4CHex)Cl_2]$ [32]} and the smallest angle with N11. The copper(II) center is displaced out of the basal plane toward Cl2 and the basal plane is at an angle of 9.61(0.20)° to the thiosemicarbazone moiety. The thiosemicarbazone moiety and the pyridine ring are nearly coplanar as found for the previously discussed $[Fe(Ampip)_2]ClO_4$.

A comparison of the copper(II)–thiosemicarbazone ligand bond distances shows that the bonds to copper(II) by S1, N12 and N11 in $[Cu(HAmpip)Cl_2]$ are shorter than these bonds in $[Cu(HBz4P)Cl_2]$ [3] and $[Cu(HFo4CHex)Cl_2]$ [32] indicating the present complex to be more strongly coordinated. Compared to $[Cu(HBz4P)Cl_2]$ and $[Cu(HFo4CHex)Cl_2]$ the S1–C17 bond is longer and the C16–N12 bond shorter in $[Cu(Ampip)Cl_2]$. Of interest in $[Cu(Ampip)Cl_2]$ is that the bond to the amide function, C16–N15, is the second shortest C–N bond in the ligand indicating considerable electron donation to the thiosemicarbazone function by this group. This is presumably the reason for the stronger ligand field for the 2-pyridineformamide thiosemicarbazones compared to other heterocyclic thiosemicarbazones. As would be expected the other bond distances of the thiosemicarbazone moiety also vary to some extent in the aforementioned three complexes. The most noticeable difference is N12–N13, which is nearly 0.05 Å longer in $[Cu(Ampip)Cl_2]$ compared to $[Cu(HBz4P)Cl_2]$ [3] and $[Cu(HFo4CHex)Cl_2]$ [32]. The Cu–S1–C17, Cu–N12–C16 and Cu–N12–N13 bond angles in $[Cu(Ampip)Cl_2]$ are essentially the same as found for $[Cu(HFo4CHex)Cl_2]$, but very different than found for $[Cu(HBz4P)Cl_2]$ indicating the effect of bulkiness of the phenyl group attached to C16 in the latter.

The methanol molecule is not involved in hydrogen bonding with the NH_2 function in $[Cu(Ampip)Cl_2]$, which does hydrogen bond to apical chloro ligands of different neighboring molecules, Table 4. The packing units are pseudodimers in which the two molecules are mutually inverted (symmetry transformation $-x$, $-y+2$, $-z+2$); the thiosemicarbazone moieties are parallel to each other and each apical chlorine, Cl2, lies almost alongside the partner molecule, interacting with its N13 and N15 hydrogens. The Cu–Cu distance within each dimer is 6.469 Å. In contrast, $[Cu(HFo4CHex)Cl_2]$ [32] has bridging by the basal chloro ligand, Cl1, resulting in stacking of the

Table 8
Solid state electronic spectra (cm^{-1}) for HAmpip and its metal complexes

Compound	Intraligand and charge transfer	d → d
Hampip	32 340, 24 360, 22 360	
$[Fe(Ampip)_2]ClO_4$	33 560, 26 570, 21 230	11 000
$[Co(Ampip)_2]ClO_4$	33 930, 29 150, 25 920, 21 090	15 960, 11 110, 6860
[Co(Ampip)Cl]	34 350, 29 790, 22 020	16 530, 11 190, 6950
[Cu(Ampip)OAc]	32 620, 30 460, 23 570	17 660
[Cu(Ampip)Cl]	31 730, 29 430, 23 390, 20 320	17 050
$[Cu(HAmpip)Cl_2]$	31 680, 28 490, 22 260	17 520, 14 010

molecules in an 'eclipsed' arrangement and [Cu(HBz4P)Cl_2] [3] also has bridging by the basal chloro ligand to form a dimer but each Cl2 interacts weakly with N(3)H and N(4)H of an adjacent dimer resulting in a weak chain of dimers and a 'non-eclipsed' packing pattern.

The electronic spectrum shows that the $n \rightarrow \pi^*$ band associated with the pyridyl ring and imine function (i.e. 31 680 cm^{-1}) does not shift significantly from its position in the spectrum of HAmpip, but the band due to the thioamide portion of the molecule shifts to higher energy by approximately 5000 cm^{-1}. The shoulder at 22 260 cm^{-1} is due to a $S \rightarrow Cu(II)$ charge transfer band. The powder ESR spectrum of [Cu(HAmpip)Cl_2] is consistent with a $d_{x^2-y^2}$ ground state and has a slight rhombic appearance consistent with unequal coordination distances about the basal plane. Averaging g_2 and g_3 to be $g_\perp$ and assigning 17 520 cm^{-1} to $^2B_{1g} \rightarrow {}^2E_g$ and 14 010 cm^{-1} to $^2B_{1g} \rightarrow {}^2B_{2g}$ allows calculation of $k_\perp = 0.64$ and $k_\parallel = 0.57$. Thus, there is considerable covalent character to the coordinate bonds, consistent with coordination of two chloro ligands and a sulfur, and in-plane π-bonding is more important than out-of-plane π-bonding [33].

3.5. [Cu(Ampip)OAc]and [Cu(Ampip)Cl], spectral characterization

These two complexes have similar IR spectra with decreases of approximately 16 cm^{-1} for ν(C=N) and approximately 88 cm^{-1} for ν(CS) and an increase of 22 cm^{-1} for ρ(py) compared to the spectrum of HAmpip indicating coordination of the pyridine nitrogen, imine nitrogen and thiolato sulfur atoms. The spectrum of [Cu(Ampip)Cl] shows a strong band at 307 cm^{-1} assignable to ν(CuCl); the low energy of this band compared to the usual energy of approximately 335 cm^{-1} [34] for a terminal chloro ligand suggests significant bridging to neighboring copper(II) centers. Their electronic spectra are also similar with the $d \rightarrow d$ band maxima for [Cu(Ampip)OAc] being marginally higher in energy. However, the ESR spectra of the two complexes are different; the less covalent oxygen donor of the acetato ligand results in a higher g_1 for [Cu(Ampip)OAc] than for [Cu(Ampip)Cl]. Also, the lower value of g_1 for [Cu(Ampip)Cl] than found for [Cu(HAmpip)Cl_2] is consistent with weaker axial bonding in the former.

3.6. [Zn(HAmpip)Br_2], structural and spectral characterization

[Zn(HAmpip)Br_2] (Fig. 5), like [Cu(HAmpip)Cl_2], crystallizes in the triclinic crystal system with $P\bar{1}$ symmetry and two molecules in the unit cell. The bonds from HAmpip to zinc are longer than the corresponding bonds in [Cu(HAmpip)Cl_2], which results in S1–C17 and C16–N12 being shorter, although this difference is about their combined e.s.d. values. The S1–Zn–N11 angle is much smaller than the corresponding angle in [Cu(HAmpip)Cl_2] and when α and β are assigned to N11–Zn–S1 and Br2–Cu–N2 angles, respectively, $\tau = 0.25$. This value indicates considerable distortion toward trigonal pyramid stereochemistry and is much more distorted than [Zn(HAm4DH)Br_2] ($\tau = 0.04$), where HAm4DH is 2-pyridineformamide thiosemicarbazone [5]. The two Zn–Br bond distances in [Zn(HAmpip)Br_2] are comparable to those of [Zn(HAm4DH)Br_2], but Zn–S is significantly shorter, 2.416(3) Å compared to 2.4744(13) Å indicating the greater electron density available due to the presence of the azacyclo function compared to NH_2. The Zn–N distances of the two complexes are more similar although Zn–N11 is shorter and Zn–N12 longer for [Zn(HAmpip)Br_2], which is unusual for heterocyclic thiosemicarbazone complexes.

N13*H13* interacts with the DMSO oxygen, as does one of the NH_2 hydrogens, H15A, and the latter is a the stronger of the two interactions. Also, H15A is at a distance from the DMSO sulfur suggesting some interaction; the non-bonding N15···S22 distance is similar to that found for heterocyclic thioureas [22]. The second NH_2 hydrogen, H15B, interacts with a bromo ligand on a neighboring molecule. The hydrogen bonding in [Zn(Ampip)Br_2] and [Zn(HAm4DH)Br_2] is similar, but more extensive in the latter because of the additional NH_2 function. Zn is displaced from the Br2–S1–N12–N11 basal plane by 0.6339(27) Å toward Br1, this large distance further indicating the distortion from square pyramid stereochemistry. The thiosemicarbazone moiety has a mean plane deviation of 0.0211 Å compared to 0.0500 Å for HAmpip and forms an angle of 2.64(98)° with the mean plane of pyridine ring compared to 11.95(13)° for HAmpip.

The infrared spectrum of [Zn(HAmpip)Br_2] exhibits a large number of bands in the ν(NH) region, and the medium band assigned to $\delta(NH_2)$ (1663 cm^{-1}) remains in the same position as in HAmpip. In addition, the increase of the ν(C=N) (from 1601 to 1617 cm^{-1}), decrease of 10 cm^{-1} for ν(CS) and increase of 31 cm^{-1} for ρ(py) compared to HAmpip is consistent with coordination of the pyridine and imine nitrogen atoms as well as the thione sulfur atom. Coordination by the imine nitrogen causes a shift of ν(NN) from 1006 to 1015 cm^{-1}. In the ^1H NMR spectrum of [Zn(HAmpip)Br_2] the presence of all the peaks found in the spectrum of HAmpip confirms non-deprotonation and coordination by the thione sulfur atom is reflected by a deshielding of N3H (from 12.69 to 10.39 ppm). In the ^{13}C NMR spectrum the C6 signal is shifted downfield (from 143.67 to 144.77 ppm), while the C7 signal is shifted upfield (from 178.43 to 175.89 ppm).

4. Conclusions

Based on bond distances and spectral values, HAmpip (or Ampip) in the complexes discussed here provides a stronger ligand field than its analogs prepared from 2-formylpyridine, 2-acetylpyridine and 2-benzoylpyridine [1–3]. This is consistent with our findings with complexes of HAm4M in a similar comparison and suggests that thiosemicarbazone moieties attached to amide carbons could provide a series of compounds with greater pharmaceutical promise than previously studied thiosemicarbazones [4]. The National Cancer Institute and others [4] have evaluated a large number of thiosemicarbazones, but amide thiosemicarbazones have not been tested to date.

5. Supplementary material

Crystallographic data for the structural analysis have been deposited with the Cambridge Crystallographic Data Centre, CCDC Nos. 154845, 160136–160138 for compounds $C_{24}H_{32}N_{10}O_4S_2ClFe$, $[Fe(Ampip)_2]ClO_4$; $C_{13}H_{21}Cl_2CuN_5OS$, $[Cu(HAmpip)Cl_2]\cdot CH_3OH$; $C_{14}H_{22}Br_2N_5OS_2Zn$, $[Zn(HAmpip)Br_2]\cdot DMSO$ and $C_{12}H_{17}N_5S$, HAmpip. Copies of this information may be obtained free of charge from The Director, CCDC, 12 Union Road, Cambridge, CB2 1EZ, UK (fax: +44-1223-336033; e-mail: deposit@ccdc.cam.ac.uk or www: http://www.ccdc.cam.ac.uk).

Acknowledgements

Acknowledgement is made to the Donors of the Petroleum Research Fund, administered by the American Chemical Society, for the partial support of this research.

References

[1] D.X. West, C.E. Ooms, J.S. Saleda, H. Gebremedhin, A.E. Liberta, Transition Met. Chem. 19 (1994) 553 (and references therein).
[2] D.X. West, H. Gebremedhin, R.J. Butcher, J.P. Jasinski, A.E. Liberta, Polyhedron 12 (1993) 2489 (and references therein).
[3] D.X. West, J.S. Ives, J. Krejci, M.M. Salberg, T.L. Zumbahlen, G.A. Bain, A.E. Liberta, J. Valdés-Martínez, S. Hernández-Ortega, R.A. Toscano, Polyhedron 14 (1995) 2189.
[4] (a) M.C. Miller, C.N. Stineman, J.R. Vance, D.X. West, I.H. Hall, Anticancer Res. 18 (1998) 4131;
(b) M.C. Miller, C.N. Stineman, J.R. Vance, D.X. West, I.H. Hall, Appl. Organomet. Chem. 13 (1999) 9.
[5] A. Castiñeiras, I. Garcia, E. Bermejo, D.X. West, Z. Naturforsch., Teil B 55 (2000) 511.
[6] A. Castiñeiras, I. Garcia, E. Bermejo, D.X. West, Polyhedron 19 (2000) 1873.
[7] A. Castiñeiras, I. Garcia, E. Bermejo, K.A. Ketcham, D.X. West, submitted for publication.
[8] A. Castiñeiras, I. Garcia, E. Bermejo, K.A. Ketcham, D.X. West, submitted for publication.
[9] D.X. West, J.K. Swearingen, A.K. El-Sawaf, Transition Met. Chem. 25 (2000) 87.
[10] D.X. West, J.K. Swearingen, J. Valdés-Martínez, S. Hernández-Ortega, A.K. El-Sawaf, F. van Meurs, A. Castiñeiras, I. Garcia, E. Bermejo, Polyhedron 18 (1999) 2919.
[11] A. Castiñeiras, I. Garcia, E. Bermejo, K.A. Ketcham, A.K. El-Sawaf, D.X. West, Z. Anorg. Allg. Chem., in press.
[12] K.A. Ketcham, I. Garcia, J.K. Swearingen, E. Bermejo, A.K. El-Sawaf, A. Castiñeiras, D.X. West, in preparation.
[13] J.P. Scovill, Phosphorus, Sulfur Silicon 60 (1991) 15.
[14] J. van Koningsbruggen, J.G. Haasnoot, R.A.G. De Graaff, J. Reedijk, Inorg. Chim. Acta 234 (1995) 87.
[15] Bruker, SMART and SAINT. Area Detector Control and Integration Software. Bruker Analytical X-ray Instruments, Inc. Madison, WI, USA, 1997.
[16] G.M. Sheldrick, SADABS. Program for Empirical Absorption Correction of Area Detector Data. University of Göttingen, Göttingen, Germany, 1997.
[17] G.M. Sheldrick, Acta Crystallogr., Sect. A 46 (1990) 467.
[18] G.M. Sheldrick, SHELX-97. Program for the Refinement of Crystal Structures, University of Göttingen, Germany, 1997.
[19] International Tables for X-ray Crystallography, vol. C, Kluwer Academic, Dordrecht, The Netherlands, 1995.
[20] A.L. Spek, PLATON. A Multipurpose Crystallographic Tool, Utrecht University, Utrecht, The Netherlands, 1999.
[21] D.X. West, G.A. Bain, R.J. Butcher, J.P. Jasinski, Y. Li, R.Y. Pozdniakiv, J. Valdés-Martínez, R.A. Toscano, S. Hernández-Ortega, Polyhedron 15 (1996) 665.
[22] (a) D.X. West, J.K. Swearingen, A.K. Hermetet, L.J. Ackerman, C. Presto, J. Mol. Struct. 522 (2000) 27 (and references therein);
(b) D.X. West, J.K. Swearingen, A.K. Hermetet, L.J. Ackerman, J. Mol. Struct. 562 (2001) 95.
[23] (a) D.X. West, I.S. Billeh, G.A. Bain, J. Valdés-Martínez, K.H. Ebert, S. Hernández-Ortega, Transition Met. Chem. 21 (1996) 572;
(b) D.X. West, P.M. Ahrweiler, G. Ertem, J.P. Scovill, D.L. Klayman, J.S. Flippen-Anderson, R. Gilardi, C. George, L.K. Pannell, Transition Met. Chem. 10 (1985) 264.
[24] W.J. Geary, Coord. Chem. Rev. 7 (1971) 81.
[25] C.A. Reed, T. Mashiko, S.P. Bentley, M.E. Kastner, W.R. Scheidt, G. Spartalian, G. Lang, J. Am. Chem. Soc. 101 (1979) 2948.
[26] (a) Y. Nishida, A. Sumita, K. Hayashida, H. Oshima, S. Kida, Y. Maeda, J. Coord. Chem. 9 (1979) 161;
(b) N. Matsumoto, K. Kimoto, K. Nishida, A. Ohyoshi, Y. Maeda, Chem. Lett. (1984) 479.
[27] D.X. West, B.L. Mokijewski, H. Gebremedhin, T.J. Romack, Transition Met. Chem. 17 (1992) 384.
[28] C. Maichle, A. Castiñeiras, R. Carballo, D.X. West, H. Gebremedhin, M.A. Lockwood, C.E. Ooms, T.J. Romack, Transition Met. Chem. 20 (1995) 228 (and references therein).
[29] D.X. West, D.S. Galloway, D.A. Case, Transition Met. Chem. 13 (1988) 415.
[30] D.X. West, J.P. Jasinski, J.M. Jasinski, R.J. Butcher, J. Chem. Crystallogr. 29 (1999) 1089 (and references therein).
[31] A.W. Addison, T.N. Rao, J. Reedijk, J. van Rijn, C.C. Verschoor, J. Chem. Soc., Dalton Trans. (1984) 1349.
[32] D.X. West, J.K. Swearingen, T.J. Romack, I.S. Billeh, J.P. Jasinski, Y. Li, R.J. Staples, J. Mol. Struct. 570 (2001) 129.
[33] B.J. Hathaway, Structure and Bonding, vol. 4, Springer, Berlin, 1973, p. 60.
[34] G. DeVoto, M. Massacesi, R. Pinna, G. Ponticelli, Spectrochim. Acta 38A (1982) 725.